ORIGINAL ARTICLE

Journal Section

Role of chlorine, bromine, iodine, and dehalogenation in the fluorinated small molecule Y6 for highly efficient organic solar cells.

A. Romo-Gutiérrez[1] | Z. N. Cisneros-García[1] | J. G. Rodríguez-Zavala[1*]

[1]Departamento de Ciencias Exactas y Tecnología, Centro Universitario de los Lagos, Universidad de Guadalajara, Lagos de Moreno, Jalisco, 47463, Mexico.

Correspondence
J. G. Rodríguez-Zavala, Departamento de Ciencias Exactas y Tecnología, Centro Universitario de los Lagos, Universidad de Guadalajara, Lagos de Moreno, Jalisco, 47463, Mexico.
Email: jgrz@culagos.udg.mx

Funding information
Fellowship from the Mexican National Council of Science and Technology (CONACYT) [application no. 741373], Universidad de Guadalajara [Pro-SNI-2020].

In a recent experimental investigation, the chlorination of the highly efficient Y6 fluorinated molecule improved up to 16.5 % the power conversion efficiency of an organic solar cell. To understand the better performance of BTP-4Cl:PBDB-TF acceptor-donor combination in comparison with BTP-4F:PBDB-TF in the newly reported organic solar cell, DFT calculations were performed in order to obtain a diversity of parameters related to molecular properties, such as electroacceptance, electron energy levels, absorption spectrum, charge mobility, and kinetics in exciton dissociation/recombination processes. Interestingly, chlorination improves charge mobility and the capacity to accept electrons. The binding energy is lower for the chlorinated than the fluorinated molecule, revealing an easier exciton cleavage in the former. Absorption spectra are in line with experimental ones, suggesting an excellent donor-acceptor complementarity. Additionally, novel molecules were proposed taking into account synthesized compounds, and the same parameters were analyzed. Results showed exciting behavior for the theoretically suggested compounds. Many properties were improved with the proposed molecules, which can also be exploited in solar photocells. Although it is a challenge to simulate/model a complete photoactive layer of an organic solar cell, it is proved through electronic structure calculations that the properties of the materials involved in the photovoltaic device can be obtained. In this way, give some light on the power conversion efficiency comparison and propose new compounds.

KEYWORDS
DFT calculations, Photovoltaic Parameters, Organic Solar Cells

1 | INTRODUCTION

As a result of the increasing global energy demand, photovoltaic solar energy has become one of the most promising renewable energy alternatives [1, 2]. The photovoltaic devices are divided mainly into inorganic, organic, and hybrid solar cells. Although inorganic cells are still more efficient, these kinds of artifacts are also more expensive, which represents a vital barrier [3]. On the other hand, organic solar cells (OSC) have become a very favorable alternative to inorganic silicon-based solar cells [4, 5, 6, 7]. OSC offers the benefits of low production cost, lightweight, flexibility, transparency, and high production control, which in turn represents some implementation advantages[8, 9, 10, 11]. Whereas a few years ago, the most common organic solar cells were based on fullerenes, in recent years, the highest efficiencies have been found in cells without fullerenes or non-fullerene solar cells [12]; in fact, regarding OSC, the current top in the power conversion efficiency (PCE) was reached mainly by small molecules (SM) and polymer-based devices [12, 13, 14].

Non-fullerene n-type organic semiconductors have attracted significant attention due to their great potential as acceptors in photovoltaic cells [15]. Specifically, in 2019 it was synthesized an acceptor molecule that employs a ladder-type electron-deficient-core-based central fused ring (di-thienothiophen[3.2-b]-pyrrolobenzothiadiazole) with a benzothiadiazole (BT) core to fine-tune its absorption and electron affinity. This is an end fluorinated molecule and is known as Y6 (see Fig. 1) [16]. Fluorination was of great importance due to several characteristics of these compounds (down-shifted highest occupied molecular orbital [HOMO] and lowest unoccupied molecular orbital [LUMO], increased intermolecular and intramolecular interactions, high polarization, and low coulombic potential between holes and electrons), which resulted in increased PCE [17]. Later, a new (chlorinated) acceptor-donor-acceptor (A-D-A) type small-molecule acceptor, NCBDT-4Cl, was reported, showing wide and efficient absorption ability in the range of 600–900 nm with a narrow optical bandgap of 1.40 eV [18]. On the other hand, Zhang *et al.* [19] showed that chlorination had more capacity to lower molecular energy levels and broaden the absorption spectrum in comparison with fluorination, which allows an increase in the PCE. Additionally, since chlorination is easier than fluorination synthesis, material costs decrease, which benefits large-scale production.

Recently, Cui *et al.* [20] synthesized a chlorinated low-bandgap acceptor, BTP-4Cl, by replacing the halogen atoms of the fluorinated acceptor Y6, called BTP-4F. According to their report, LUMO showed a decrease, owing to chlorination [19, 21], however an increase in open-circuit voltage is obtained unexpectedly. Additionally, a series of experimental parameters were improved, including the non-radiative energy loss, contributing to the enhancement in open-circuit voltage. Furthermore, an extended optical absorption was produced by chlorination, which contributed in the same way to the increase in PCE, going from 15.6 % for BTP-4F compound to 16.5 % for BTP-4Cl compound, both using the same donor polymer PBDB-TF and an area of 0.09 cm^2 per independent cell. These high PCE values placed these photovoltaic materials among the top devices for single-junction organic photovoltaic (OPV) cells.

In addition to the broadening of optical absorption through chlorination, there are factors directly related to the electronic structure of photovoltaic materials that impact the PCE. Thus, even though it is no possible to model or simulate an entire experiment, it is viable to obtain valuable information from theoretical calculations [22, 23, 24].

The dipole is an indicator of electron distribution. A low dipole moment favors conduction because it indicates a greater delocalization of electrons [25]; in addition, it has an inverse relationship with the mobility of charge carriers [26]. After exciton is created, it is dissociated at the donor/acceptor interface of the photoactive layer, for which it is convenient to have materials that are quality acceptors and donors in this layer to efficiently carry out the separation of the exciton [27]. The binding energy is another crucial factor in the efficiency of a photocell. The smaller the binding energy, the easier the exciton dissociation [28]. Reorganization energy is related to the transport process in molecules. Therefore, this amount provides essential information for the proper functioning of a photocell [29]. HOMO and

LUMO position for donor and acceptor is prime because it is related to open-circuit voltage; more precisely, this parameter depends on the energy difference between HOMO of donor and LUMO of acceptor [30]. On the other hand, the LUMO offset between donor and acceptor should be well controlled to be of considerable size to provide enough energetic driving force for efficient charge separation to minimize the energy loss [31, 32].

From an experimental point of view, several parameters like open-circuit voltage (V_{OC}), short-circuit current (J_{SC}), and fill factor (FF) are relevant to obtain a good performance in solar cells. Additionally, many of these experimental parameters are associated with the electronic structure of materials used in the organic photovoltaic (OPV) device, concretely in the photoactive layer.

In the particular case of Cui *et al.*, chlorination of Y6 broadens the absorption spectrum and modifies the frontier molecular orbitals. However, while the former undoubtedly improves the PCE, the latter unexpectedly also enhances it. Even though chlorination lowers the position of the frontier molecular orbitals, which could result in a V_{OC} decrease, the F $\rightarrow$ Cl exchange resulted in a V_{OC} increase, and finally, an increase in PCE. Nevertheless, as will be seen in this report, chlorination not only broadens the absorption spectrum but also improves several parameters related to the electronic structure, such as the ability to accept/donate electrons, charge transfer/mobility, and exciton dissociation. Improvement of several of these parameters can demonstrate the enhancement of PCE in PBDB-TF:BTP-4Cl compared to PBDB-TF:BTP-4F junction. In addition, also from a theoretical point of view, here was observed that the following halogenation, Cl $\rightarrow$ Br, once again improves all these parameters, which results in an engaging novel proposal to continue increasing the PCE. Even the substitution by iodine proposes parameters comparable to those obtained with fluorine. In this way, motivating results are achieved from the proposed systems.

This paper is organized as follows: in the next section, details of computational calculations are shown. Additionally, in the supporting information, the justification of our methodology is extended. After that, results and discussion are presented. Finally, conclusions are stated in the last section.

2 | COMPUTATIONAL DETAILS

In order to have a better description of the molecules, a total of five different exchange-correlation potentials (XC-functionals) and up to nine different basis sets were tested (see supporting information). Our theoretical frontier molecular orbital energies were compared with their experimental analogs obtained in [20] employing square-wave voltammetry to find the most reliable method of calculation. In a first step, molecules were optimized with all exchange-correlation potentials and the 6-31G** basis set. The results of each XC-functional were compared with the experimental reference values, and the most accurate functional was selected. After the XC-functional selection, molecular geometries were reoptimized using the nine proposed basis sets, and HOMO-LUMO frontier orbital energies were compared anew, with the experimental reference values. It is worth mentioning that the vibrational frequencies were obtained for all optimized geometries to corroborate that each structure was at a minimum of the potential energy surface. Among all theory frameworks (see supporting information), the HSE [33] hybrid exchange-correlation potential and the 6-311G** [34] triple zeta basis set showed the minimum difference concerning the experimental HOMO-LUMO energies reported by Cui *et al.* Given the above mentioned, the HSE potential and the 6-311G** basis set were the natural selection to carry out the present work. Lastly, we are conscious that the size of the iodine atom is more significant than the rest. Therefore, for this atom we used the Def2-TZVP triple zeta valence basis set proposed by Ahlrichs and coworkers [35, 36], which is a good compromise between computational cost and accuracy.

All geometry optimizations, vibrational frequencies, single point, and excited-state calculations, as well as the inclusion of the solvent effect with the solvation model based on density (SMD) [37] were performed in the well-known

computational chemistry package Gaussian16 [38]. In contrast, exciton binding energies and transition distributions were obtained with the Multiwfn software [39].

Molecular structures of acceptors BTP-4X (X = F, Cl) and donor PBDB-TF are shown in Figure 1, and the optimized geometries of the proposed compounds BTP-4Br and BTP-4I, as well as the nonhalogenated system BTP-4H, can be observed in Figure 2. Lateral alkyl chains 2-ethylhexyl and undecyl were replaced with methyl groups to reduce the computational cost; as has been discussed in other reports, the influence of these aliphatic chains does not significantly affect the electronic structure [40, 41]. Regarding the donor PBDB-TF, all calculations were performed on one unit of the polymer. Including more units (up to four), a meaningful difference between theoretical and experimental frontier orbital energies was found, especially in the case of the HOMO (see the supporting information).

Finally, to complete the description of the methodology, the charge transfer descriptors, reorganization energies, and exciton binding energy are briefly described in the supporting information.

3 | RESULTS AND DISCUSSION

3.1 | Dipole moment

Dipole is an indicator of electron density distribution. A low dipole moment favors semiconduction because it indicates greater electron delocalization [25], in addition to being inversely proportional to mobility of charge carriers [26].

Table 1 shows, in light cyan, values of dipole moment of the two acceptors experimentally studied by Cui *et al.* calculated in gas phase (GP), chloroform (CF), and chlorobenzene (CB). As can be seen, BTP-4Cl is the molecule with the lowest dipole moment in gas phase and chloroform, then, it is possible to argue it is also the one with the highest delocalization of electron density and mobility of charge carriers on its surface. Such assertions in gas phase and chloroform are consistent with the better experimental performance of PBDB-TF:BTP-4Cl. On the other hand, the value of dipole moment in chlorobenzene is reversed, which would lead to a situation that is not so favorable for the transport of charge in this solvent.

Another promising finding was that the proposed BTP-4Br molecule is the one with the lowest dipole moment in the three phases (see Table 1). In calculations without solvent, its dipole is only two-thirds of its BTP-4Cl counterpart. The conjecture that is reached is that BTP-4Br could show excellent delocalization of electron density thanks to the extraordinarily low magnitude of its dipole. Such assertion could be explained by the possible equilibrium between the length of the C–Br bond, its moderate covalent radius and the electronegativity of bromine, which is less than 3 points on the Pauling scale (against 3.16 for chlorine and 3.98 for fluorine) [42]. This aspect would have a positive effect on its semiconductor character and its ability for the mobility of charge carriers. In addition, the same table reveals there is a significant increase of dipole moment in solvent phases, except in the already mentioned system with Br.

The other proposed acceptor, BTP-4I, exhibits a dipole moment slightly lower than that of its fluorinated counterpart in the solvent-free medium, but higher when solvents are taken into account. It is not wise here to speak of a hint of a hypothetical improvement in semiconduction-related properties. Finally, the halogen-free acceptor is the one with the highest values of the referred parameter, with more than 5 debyes in the gas phase and exceeding 8 in solution. The negative consequences of dehalogenation did become evident in this area.

3.2 | Charge transfer descriptors

Donating and accepting charge are two key processes in the operating principle of photovoltaic devices. As it is well known, Density Functional Theory (DFT) has been widely used to obtain the donor or acceptor capacity. In the present work, so as to get deep insight into the donating-accepting character, different indicators such as I, A, ω^+, ω^-, χ^+, and χ^- were calculated. Here is important to mention that, the lower I, ω^-, and χ^-, the better donating character has the molecule, and by the other hand, as the higher A, ω^+, and χ^+ are, the better acceptor capacity.

According to results shown in Table 2, in regard to electron affinity (A) and ionization potential (I) calculated in gas phase, it is possible to observe that in a consistent way the electron affinity index is higher for both acceptors experimentally studied (highlighted in light cyan in Table 2) compared to the donor compound (highlighted in yellow) and the ionization potential is lower for the donor. Interestingly, BTP-4Cl is better acceptor than BTP-4F according to all A, ω^+, and χ^+ indicators.

With the purpose of resemble the experiment, the above mentioned indicators were calculated including the solvent effect through the solvation model based on density (SMD). Both chloroform and chlorobenzene were modeled by SMD method; interestingly, the same tendencies were observed, it is, also the electron affinity is higher in BTP-4Cl as well as ω^+ and χ^+. These theoretical results shed some light on explaining the experimental results reported in [20], where the photovoltaic system formed by a photoactive layer with the PBDB-TF donor and the BTP-4Cl acceptor has a better efficiency than the system formed by a photoactive layer with the same donor and BTP-4F acceptor.

In gas phase, none of the proposed molecules (BTP-4Br, BTP-4I, and BTP-4H) exhibits an increase in electron charge acceptance property with respect to BTP-4F or BTP-4Cl, and in the presence of solvents the situation changes a little. In chlorobenzene, for example, BTP-4Br would seem to be the best electroacceptor system because it has χ^+ = 16.61 eV and ω^+ = 9.71 eV, which are slightly higher values, especially ω^+, than those of the chlorinated system. In chloroform, on the other hand, parameters that define the acceptor character of molecules are almost identical for the compound postulated with bromine and the well-known chlorinated system. While χ^+ for BTP-4Br is greater by only 10 meV, ω^+ is less by 20 meV in the brominated system compared to the chlorinated one, moreover electron affinity is the same for both compounds, which corroborates the equality in the acceptor capacity of both acceptor compounds.

BTP-4I, although not dazzling, does improve the numbers of BTP-4F in solution. In both solvents, the iodinated acceptor prevailed over the fluorinated one for the three indices that measure the electroacceptor ability. These theoretical results make us suspect that the proposed systems could well compete with BTP-4F and BTP-4Cl systems in the separation of negative charge carriers and be a viable option for their application in bulk heterojunction organic solar cells.

BTP-4H is the worst acceptor of all, which accentuates the deficiency due to dehalogenation that has been envisioned throughout the study.

3.3 | Reorganization energies

In the process of transporting charge, the molecules of photoactive zone undergo structural adjustments. Some examples of these adjustments are the passage of a geometry electrically neutral to a cationic or anionic and the reverse case. The reorganization energy is related to the activation energy that supposes the global reaction of electron transfer; having said that, it is natural to think that the reorganization energy should ideally be minimum, because thus the kinetics of the transfer is maximum (faster) [43, 44]. Reorganization energies for holes and electrons of the six molecules under study in gas phase, chloroform, and chlorobenzene are shown in the Table 3.

Reorganization energy comprises the contributions belonging to electrons (λ_-) and those relating to holes (λ_+). As can be seen in Table 3, λ_- is considerably lower than λ_+ in the two acceptors, which gives an idea of which type of charge carrier is more likely to transit on its surface. On the contrary, λ_+ dominates in the field of PBDB-TF, which suggests the preference that this system has for the transport of holes (or, in other words, the donation of electrons). A very interesting point to highlight in this table is the comparison between the two acceptors experimentally studied, where lower λ_- is clearly observed in the chlorinated compound compared to the one with F in gas phase and solvents. This last result indicates that, following the same theoretical interpretation, BTP-4Cl is a better electron transporter system and contributes to a better performance in the photoactive film, which is in line with the experiment and preliminary estimates.

In the solvent-free medium, reorganization energy belonging to the negatively charged carriers for BTP-4Br and BTP-4I acceptors is 0.126 eV, a value which is lower than 0.134 eV of BTP-4F, but it is above 0.123 eV of BTP-4Cl. In solvents, λ_- of BTP-4Br is 0.101 eV and 0.099 eV in chloroform and chlorobenzene, respectively. These amounts are below their BTP-4Cl and BTP-4F counterparts. Likewise, BTP-4I also has a λ_- in solution that is lower than that of systems with fluorine and chlorine. This numerical assessment has a positive impact on our reflection on the possible semiconductor properties of the suggested systems and their implications in photovoltaic devices. From the quantitative perspective given in this work, the capacity that BTP-4Br and BTP-4I would have in transport of electron charge on their surface is promising.

3.4 | Binding energies

In order to carry out an effective photovoltaic process that generates electrical energy from absorption of light is necessary to dissociate the exciton, freeing the hole and electron in the photoactive layer. Exciton binding energy (E_b) is the indicator of the feasibility for such separation to occur. Since binding energy is related to the coulombic attractive force between hole and electron, the smaller E_b, the greater the possibility of exciton separation.

E_b obtained for all the compounds and solvents contemplated in the present investigation can be consulted in Table 4. Comparing E_b for the two acceptor molecules (highlighted in light cyan in table) used by Cui *et al.*, it is observed that the compound with Cl has a lower binding energy regardless of the type of calculation (gas phase or with solvents). This would indicate a lower energy required to separate charges and due to this a better efficiency of photoactive layer.

Exciton binding energy turned out to be smaller for both proposed compounds (BTP-4Br and BTP-4I) than that of molecules investigated by Cui *et al.* This observation is generalized for gas phase and the two solvent phases. The 2.57 eV in gas phase improves the 2.60 eV that BTP-4Cl has, which is a good sign that exciton dissociation could occur more easily in acceptors with bromine and iodine atoms. Once in solution, the difference in favor of the aforementioned remains, since there is an E_b of 2.54 eV (2.53 eV in the case of BTP-4I) against 2.57 eV for the chlorinated system.

Regarding the solvent effect, it should be noted that, in the five acceptors, there was a regular decrease in E_b of approximately 0.03 eV if we compare what is shown in gas phase with that obtained in chloroform and chlorobenzene. In addition, it can be said that results between one and another solvent remained practically identical.

3.5 | Position of frontier molecular orbitals and related properties

Frontier molecular orbitals are intrinsically linked to processes such as semiconduction and optical absorption, as well as governing some other photovoltaic parameters.

In Table 5, the congruence between the HOMO and LUMO energy obtained from experiment and the one esti-

mated theoretically can be clearly observed for both acceptors, as already highlighted in the supporting information. Energy levels of BTP-4F and BTP-4Cl are quite close, but those of BTP-4Cl are in lower positions (they are more negative), which is also in agreement with the measurements of Cui *et al.* Similarly, the donor's HOMO and LUMO orbitals are above their homologues on the acceptor molecules. This alignment is essential for the correct transfer of charge from donor to acceptor in the photoactive layer.

The poor description of donor by methodology used yielded discordant amounts that were far from experiment: HOMO-LUMO gap was positioned at 2.37 eV (ideally being between 1.3 and 1.9 eV [45]), which can be explained by the overestimation of LUMO. However, the HOMO calculated at HSE/6-311G** level agrees well with what has been reported and with what is recommended in the literature. The value obtained is close to -5.27 eV, the limit associated with the stability of a donor in an oxidizing environment such as air [40].

The driving force that guides the diffusion of the exciton is given by the energetic difference between the donor and acceptor LUMOs, $L_D - L_A$. The subtraction must be greater than 0.3 eV to achieve a successful transfer at the D-A interface [46, 47]. As can be seen, the theoretical values far exceed the minimum necessary to drive the exciton between both units. It can also be observed there is a larger energy difference between LUMO of donor and BTP-4Cl acceptor compared to the same energy difference taking into account BTP-4F acceptor. This result leads us to obtain a larger energetic driving force in system with Cl, which is required to separate the exciton into free charge carriers during the interface charge transport process. Therefore, a better charge separation process is expected in the system with Cl than in the system with F.

Position of acceptor-HOMO and donor-LUMO has a great influence on open-circuit voltage (V_{OC}), a factor that directly affects the efficiency of the photovoltaic device. A model proposed by Scharber *et al.* [30] empirically estimates V_{OC} by means of Eq. 1:

$$V_{oc} = \left(\frac{1}{e}\right)(|\varepsilon_{HOMO}^{donor} - \varepsilon_{LUMO}^{acceptor}|) - 0.3V. \tag{1}$$

Results of application of Scharber's formula to data previously exposed and its contrast with that determined by square-wave voltammetry are shown in Table 6.

A consequence of trying to improve the short-circuit current density (J_{SC}) is a possible detriment in V_{OC} due to the modification in position of orbitals and in the properties that determine the absorption of light. In general, the increase of one parameter leads to the decrement of the other, so finding a balance that maximizes the simultaneous values between V_{OC} and J_{SC} is of utmost importance. In this study, as expected, open-circuit voltage decreased for BTP-4Cl:PBDB-TF combination because LUMO of BTP-4Cl increased in magnitude. This phenomenon does not converge with information provided by Cui *et al.*, since they found a surprising increase in V_{OC} in the photocell built with the new acceptor. Here it is worth mentioning that even for them this result was unexpected, as mentioned in [20]. On the other hand, it is important to note the great description of Schaber's model and theory used, since open-circuit voltages obtained experimentally and theoretically (see Table 6) differ only in quantities less than 100 mV.

Energy of frontier molecular orbitals were also calculated for all molecules under study. Results are concentrated in Table 7. In gas phase, a slightly smaller HOMO-LUMO gap (E_g) was obtained in BTP-4Br than in BTP-4Cl, which would indicate that, in the former, photovoltaic effect would be more benefited. It is easier, of course, for an incident photon to promote an electron from ground to excited state if it must overcome a barrier of 1.62 eV rather than one of 1.65 eV. This theoretical improvement in brominated compound becomes even more extensive when analyzing E_g in chloroform and chlorobenzene. On the other hand, BTP-4I also deserves to be highlighted in this area. Position of its orbitals is very similar to what BTP-4F exhibits, nevertheless, it has a slightly smaller gap. Up to now, it is possible to

say that proposed systems have shown very favorable values of parameters associated with their electronic structure.

Another point to note is the difference between energy calculated before and after considering solvent. Decrease of approximately 0.2 or 0.3 eV in magnitude of HOMO and LUMO, as well as decrease of a few hundredths of an eV in energetic gap are noticeable in acceptor molecules. Interestingly, opposite effect was observed in donor, since HOMO energy increased in magnitude.

Contrasting with experimental data (see Table 5), energy of the two frontier molecular orbitals of BTP-4F and BTP-4Cl does not improve when including solvents, but their energy gap does. For PBDB-TF, the HOMO calculated in solution was closer to the -5.45 eV measured by Cui *et al.*, although E_g was far from that measured.

In all acceptors and solvents, the driving force, $L_D - L_A$, which aids in the diffusion of exciton from unit A to unit D of photoactive layer, was greater than 0.3 eV. Alignment of frontier molecular orbitals corresponds, in all cases, with the basic requirement that both HOMO and LUMO of donor molecule are above their homologues of acceptor species. This alignment of frontier orbitals is important for the charge transfer from donor to acceptor in the photoactive layer of the solar photocell, since when the exciton is created, the electron is attracted by the acceptor and in this way it is possible to separate the exciton. In addition, the -5.27 eV limit was also met in HOMO of PBDB-TF. This value, as already mentioned, is related to the range in which stability of this compound could prevail in the face of the effects of an oxidizing environment such as air [40].

Open-circuit voltage for the different donor-acceptor combinations and the three environments was obtained, anew, with empirical Scharber's formula. Results are shown in Table 8. One striking effect is the significant change in V_{OC} in different environments, especially when it is compared with and without solvent. It is observed that the behavior is: V_{OC} CB > V_{OC} CF > V_{OC} GP for the five combinations of acceptors with the PBDB-TF donor. This is an obvious consequence of increase in HOMO magnitude of PBDB-TF and a less negative LUMO values of the five electroacceptor systems. Furthermore, comparing with experimental data, open-circuit voltage obtained from calculations in chloroform and chlorobenzene is overestimated and is further away from that obtained in gas phase.

Finally, V_{OC} with BTP-4Br as acceptor is 0.83 V, 1.12 V, and 1.15 V in gas phase, chloroform, and chlorobenzene, respectively. All these quantities are below the other combinations in the three mediums. On the other hand, BTP-4H:PBDB-TF combination is the one that would present, from the theoretical perspective, a higher V_{OC}. Here it is worth to mention that, it is difficult to arrive at any conclusion with regard to open-circuit voltage, since on one side, in the present study a lower V_{OC} is obtained for chlorinated compound in comparison with the fluorinated one, however, experimentally Cui *et al.* unexpectedly (even so mentioned by them) found a higher V_{OC} for chlorinated system. The reason is not clear from electronic structure calculations since the lower LUMO energy of chlorinated compound would represent a lower V_{OC}.

3.6 | Absorption spectra

Absorption spectrum in ultraviolet-visible (UV-Vis) region (approximately 380-780 nm) was simulated using Time-Dependent Density Functional Theory (TD-DFT) and same methodology as applied in previous calculations (HSE/6-311G**). Ten excited states were considered.

An important aspect that must be fulfilled in the photoactive layer is the donor-acceptor complementarity, that is, for a better functioning of the photovoltaic device, donor and acceptor materials must absorb sunlight in regions (UV-Vis) that are complementary. Fortunately, this condition is satisfied for all acceptors studied here in conjunction with PBDB-TF donor. In spectrum measured by Cui *et al.*, a slight bathochromic shift of the chlorinated compound can be observed compared to the fluorinated one. Further, donor has its maximum spectrum values at lower wavelengths. As can be seen in Fig. 3(a), all these conclusions are well reproduced by the calculated spectra, albeit shifted down

around 100 nm.

Superposition of spectrum of each acceptor with that of donor covers a good part of UV-Vis and near infrared (NIR) zone, which shows a good absorption capacity of the photoactive layer and a great coupling between the two units. The slightly wider range of absorption of BTP-4Cl (given by its bathochromic shift) contributes to its excitability and, therefore, to a better use of photon harvesting. Additionally, Cui *et al.* report that BTP-4Cl has a higher molar absorption coefficient than BTP-4F [20], which is also proved through larger oscillator strenghts of BTP-4Cl compound than the fluorinated one (see Table 9).

As explained in advance, the spectroscopic data collected with TD-DFT is quite consistent with practical measurements. In the experiment by Cui *et al.*, maximum absorption peak of BTP-4F is located at 732 nm, while chlorinated acceptor is at 746 nm. Peaks derived from simulation are located correspondingly at 679 and almost 690 nm. The difference of 50-60 nm towards lower wavelengths that theory exhibits is maintained in both molecules, which reinforces the good description that methodology used provided in this area. The second and third peaks of both systems are relatively close and form a band that spans about 200 nm.

It is worth noting that Cui *et al.* report a slightly smaller optical gap for the second acceptor, which results in a lower energy requirement for electronic promotion from HOMO to LUMO and a greater probability of causing a $\pi \rightarrow \pi^*$ transition.

Electron transition analysis is essential to complement what is visually enhanced in the spectrum. Characteristics of main absorption peaks in UV-Vis region of the two experimentally studied electroacceptor molecules are presented in Table 9.

Transition with the greatest oscillator strength (f) coincides (H $\rightarrow$ L with 100 %), for the two systems, with the one associated with the maximum absorption peak, which reveals that this excited state surely captures most of the solar radiation useful to the device. In the second peak of both spectra ($\lambda \approx 603$ nm for the fluorinated system and $\lambda \approx 610$ nm for the chlorinated system) the transitions H - 1 $\rightarrow$ L (12 %) and H $\rightarrow$ L + 1 (86 %) occur, but they exhibit very weak oscillator strength.

Regarding the proposed molecules and solvents: the gas phase, chloroform, and chlorobenzene absorption spectra of the five acceptor molecules and the donor are shown in Figure 3. For simulation, 10 excited states were considered.

The good overlap of spectra of new acceptors with that of donor in the three mediums suggests that coupling in photoactive layer allows an optimal uptake of light throughout the ultraviolet, visible and near infrared region. Intersection of curves is approximately at $\lambda = 600$ nm. In general, the proposed systems have quite similar characteristics in terms of bands and peaks with the highest absorption.

In gas phase, it can be observed how the five acceptors under study present spectra with similar shapes between 300 and 900 nm. Curve of donor crosses those of acceptors at just under 600 nm.

In chloroform, the donor curve has flattened and has a small elevation around 400 nm, so its gaussian shape no longer appears in this solvent. It is clear that the absorption bands have been redshifted, resulting in an elongation of this region beyond 900 nm.

In chlorobenzene, complementarity of units D and A remains. If we combine PBDB-TF with any of the five acceptors, the coverage of both molecules within the swept area of the spectrum is evident, which leads us to suppose that light absorption could be very effective in this solvent.

Anew, analysis of electronic transitions is essential to complement what has already been said in reference to the plotted spectra. Characteristics of the three most important absorption peaks in the five electroacceptor molecules are concentrated in Tables 10 (solvent-free medium), 11 (chloroform), and 12 (chlorobenzene).

In gas phase (Table 10), novel systems BTP-4Br and BTP-4I have the maximum absorption peak at 690.38 nm

and 692.06 nm, respectively, in such a way that they have shifted slightly towards the red in relation to BTP-4F and BTP-4Cl. This displacement is consistent with the fact that electron gap is smaller in these molecules. Transition from HOMO to LUMO, with 100 %, is also the one with the highest oscillator strength, so it is possible that this is the excitation that occurs with the greatest regularity during the collection of light energy, it enhances the role they would play in the optical absorption process. BTP-4H, unlike the previous molecules, has a hypsochromic shift, since it absorbs at λ = 672.12 nm.

In all analyzed acceptors, the next two transitions of greater light absorption are very close to the transition belonging to the maximum peak, forming a band of just under 200 nm. In the second peak, the five molecules have a H → L + 1 (86 %) transition, which is the main contribution, against H - 1 → L with 11, 12 or 13 %. However, the oscillator strength is very low, barely exceeding the value of 0.05.

When the medium is chloroform (Table 11), the bathochromic shift that was detected in the spectrum was also shown numerically. Interestingly, as the mass of halogen increases, larger wavelength values are observed, with the exception of iodine. In this solvent, the point of maximum absorption of BTP-4F is located at 732.56 nm and that of BTP-4Cl almost at 746 nm. Agreement with experimental values given by Cui *et al.* is very good. Novel acceptors, meanwhile, absorb the bulk of radiation at 747.50 nm (BTP-4Br) and 745.22 nm (BTP-4I). These values are in the near infrared region, where there is a good part of light radiated by the Sun that reaches the Earth's surface [48]. Furthermore, the only transition associated with that specific wavelength in both cases is H → L (100 %) and has an f above 2.3, which suggests that electronic promotion must be carried out between HOMO and LUMO. BTP-4H shows a blueshift, with a maximum located at 724.78 nm. This is explained by its larger HOMO-LUMO gap.

In chlorobenzene, position in wavelength values for the main peak followed the sequence BTP-4Br > BTP-4Cl > BTP-4I > BTP-4F > BTP-4H. Unlike calculations in the other solvent, here the regions of the highest light absorption in BTP-4Cl and BTP-4F were not as accurate with respect to the data of experiment. However, the small difference of almost 6 nm holds for both systems. BTP-4Br and BTP-4I presented their absorption maxima at 753.19 nm and 750.38 nm, respectively. These quantities are not very different from what was obtained in chloroform, which is consistent with the fact that E_g is practically identical in both solvents. The most important peaks of BTP-4H, as happened in the two mediums previously described, were located further to the blue than those of the other acceptors.

The general effect of simulating the absorption spectrum in the UV-Vis and infrared region considering molecules in solution was the appearance of characteristic peaks and bands at wavelengths greater than those of their gas-phase counterparts. Likewise, higher values of f were obtained. The main configuration of transitions associated with each peak remained almost invariant in the three environments.

Based on what has been argued in previous paragraphs, it is speculated that photovoltaic properties of some hypothetical devices built with the two suggested (BTP-4Br and BTP-4I) acceptors could be enhanced by the position to longer wavelengths of their absorption bands and by the good coupling they have with the donor. Spectroscopic data predict that such artifacts would have a short-circuit current density that yields better efficiency.

3.7 | Exciton dissociation and recombination

Kinetics of charge transfer, that is, the study of speed at which electrons and holes are exchanged from molecule to molecule in the immediate stage of exciton cleavage, has great relevance because it makes it possible to understand what happens on the photoactive layer when a photovoltaic device is working. Monitoring of the process simultaneous or subsequent to exciton division is carried out by means of unique parameters that govern the reaction and that bear some analogy with ordinary chemical kinetics. Marcus model of charge transfer considers some parameters to understand spontaneity of this particular kind of reaction (or, in other words, the measure of how favorable it seems

in thermodynamic terms). It is also useful to predict its possible reversibility (if, on the contrary, there is a tendency towards a recombination of holes and electrons) and the hegemony manifested in one direction or another of the process.

The charge transfer (k_{CT}) and charge recombination (k_{CR}) rates can be described by Marcus model [49] in the semi-classical limit,

$$k_{CT/CR} = \sqrt{\frac{4\pi^3}{h^2 \lambda K_B T}} |V_{DA}|^2 \exp[-\frac{(\Delta G_{CT/CR} + \lambda)^2}{4\lambda K_B T}], \quad (2)$$

where k_{CT} and k_{CR} represents exciton dissociation and recombination rates, respectively, λ is the reorganization energy, h is the Planck's constant, K_B is the Boltzmann's constant, $\Delta G_{CT/CR}$ is the variation of Gibbs free energy of the reaction for exciton dissociation and recombination processes, respectively, and V_{DA} presents the electronic coupling in donor/acceptor interface.

For the aim of this work, a good description can be obtained through k_{CT}/k_{CR} quotient, therefore, according to Eq. 2, the main quantities to take into account and to perform a discussion are the variation of Gibbs free energies and reorganization energies.

Variation of Gibbs free energies for exciton recombination (ΔG_{CR}) and dissociation (ΔG_{CT}) can be obtained through [40]:

$$\Delta G_{CR} = E^{HOMO}_{donor} - E^{LUMO}_{acceptor}, \quad (3)$$

$$\Delta G_{CT} = -\Delta G_{CR} - \Delta E_{0-0} - E_b, \quad (4)$$

where ΔE_{0-0} refers to the energy of the lowest excited state of free-base donor and E_b is the binding energy. Here it is important to mention that, for an exothermic process, ΔG_{CT} and ΔG_{CR} are considered negative.

In addition, in order to calculate λ as well as dissociation and recombination rates is necessary the calculation of inner (λ_{in}) and outer (λ_{out}) reorganization energies. The former is related to geometry variations of donor (D) and acceptor (A) in the charge donating and accepting processes,

$$\lambda_{in} = \lambda_1(A) + \lambda_2(D), \quad (5)$$

where

$$\lambda_1(A) = E(A^-) - E(A) \quad (6)$$

and

$$\lambda_2(D) = E(D) - E(D^+). \tag{7}$$

Here, $E(A^-)$ and $E(A)$ are the energies of the neutral acceptor at the anionic geometry and optimal ground-state geometry, respectively, and $E(D)$ and $E(D^+)$ are the energies of the radical cation at the neutral geometry and optimal cation geometry [40]. On the other hand, λ_{out} is associated with electronic and nuclear polarization (relaxation) of the surrounding medium during the charge transfer process [31].

As a first approximation, $\lambda_{out} = 0$ was taken into account to calculate k_{CT}/k_{CR} quotient. In Table 13, λ_{in}, ΔG_{CR}, ΔE_{0-0}, ΔG_{CT}, and k_{CT}/k_{CR} quotient are shown.

Concerning the systems experimentally reported, it is easy to see the close values of λ_{in}, however, BTP-4Cl:PBDB-TF combination has lower values than BTP-4F:PBDB-TF in gas phase and chloroform, which is another factor that contribute to the better performance of chlorinated compound. In the case of proposed systems with Br, I, and H, solvents modify drastically inner reorganization energies since in gas phase this energy is larger for brominated, iodized and hydrogenated systems than fluorinated and chlorinated compounds; however, when solvents are contemplated, λ_{in} values of proposed systems are reduced, even lower than experimentally synthesized systems. It is important to remember that a low reorganization energy is related to a better charge mobility.

Even though in the calculation of dissociation and recombination rates the sum of Gibbs free energy variation with reorganization energy is very important because it appears in the exponential function, a little analysis can be made on the pure Gibbs free energy variation. Interestingly, it is easy to note that ΔG_{CR} of the fluorinated system is more negative than that of the chlorinated system regardless of the medium (GP, CF, or CB), while ΔG_{CT} is more negative for the chlorinated system than the fluorinated one, which could also be related with the better efficiency of the chlorinated system. Continuing with this type of analysis for the proposed systems, an improvement in efficiency with the brominated system could be expected due to a less negative ΔG_{CR} and a more negative ΔG_{CT} (see Table 13).

k_{CT}/k_{CR} quotient can be seen in the last column of Table 13. It is observed that BTP-4F:PBDB-TF combination has larger quotient than BTP-4Cl:PBDB-TF in all environments. This may seem a contradiction with the experimental efficiency shown by both combinations, however, we must remember that PCE depends on a synergy of several parameters where, according to the elements used in the manufacture of the photocell, some of these parameters decrease while others increase, in such a way that as a whole an attempt is made to contribute to the increase in PCE. Due to this, although in this case higher k_{CT}/k_{CR} was obtained in the fluorinated system compared to the chlorinated one, it is important to mention that most of the parameters studied in this work are better for the chlorinated system. With respect to the proposed systems, it is easy to observe that combination with hydrogenated molecule has the highest quotient, followed by BTP-4I:PBDB-TF and finally by BTP-4Br:PBDB-TF.

In addition, it is noted that k_{CT}/k_{CR} depends drastically on the medium. In gas phase the quotients are much lower than in CF and CB solvents. These results can be understood by ΔG_{CR} and ΔG_{CT} values. It can be seen that in GP the difference between ΔG_{CT} and ΔG_{CR} is smaller than in CF and CB; for example, for the fluorinated system this difference is 0.03 eV in calculation without solvent, while in CF and CB this difference is 0.61 eV and 0.66 eV, respectively. Therefore, according to

$$\frac{k_{CT}}{k_{CR}} = \exp[-\frac{(\Delta G_{CT} + \lambda)^2 - (\Delta G_{CR} + \lambda)^2}{4\lambda K_B T}], \tag{8}$$

when ΔG_{CT} is too close to ΔG_{CR}, the exponent is small, as in the case of GP. On the other side, when $|\Delta G_{CT} + \lambda| <$

$|\Delta G_{CR} + \lambda|$, $k_{CT}/k_{CR} > 1$ and vice versa. It is the reason why the gas phase has values greater than and less than one. However, in cloroform and clorobenzene, $|\Delta G_{CT} + \lambda| < |\Delta G_{CR} + \lambda|$ is always hold, and therefore $k_{CT}/k_{CR} > 1$ is kept.

The previous k_{CT}/k_{CR} quotient analysis was carried out taking into consideration $\lambda_{out} = 0$. It is well known that quantitative calculation of λ_{out} is difficult [50, 51, 52], due to this, in several previous works [53, 54, 55] a value for λ_{out} is proposed according to the characteristics of the system. However, in the present work a whole continuous variation of its value is proposed, to later carry out an analysis of the k_{CT}/k_{CR} quotient.

In Fig. 4, $\log(k_{CT}/k_{CR})$ vs λ_{out} was plotted. It was decided to plot the $\log(k_{CT}/k_{CR})$ due to the better visualization of curves in the graph scale. Furthermore, these graphs were obtained only in solvent since λ_{out} takes into account the effects of the solvent. Plots in both solvents are very similar. The height of the curves are obtained in BTP-4H > BTP-4I ≈ BTP-4F > BTP-4Cl > BTP-4Br order. At approximately $\lambda_{out} = 1$ the height of the curves is inverted, however, also at that value of λ_{out} the ratio $\log(k_{CT}/k_{CR})$ goes from being greater than one to being less than one. This would indicate that beyond that value exciton recombination would be more likely than exciton separation, which is an unwanted phenomenon. Therefore, our region of interest would be for $\lambda_{out} < 1$. Unfortunately, the k_{CT}/k_{CR} quotient in this region is not describing correctly the experimental results since theory predicts BTP-4F as a better compound than BTP-4Cl to perform the exciton dissociation in comparison with exciton recombination.

Anew, it is expected that a set of parameters holds with a synergy in order to enhance the power conversion efficiency. Therefore, on one side, in spite of some parameters get not favorable results to increase the PCE, on the other side, the rest of the parameters can be helpful to rise the PCE.

4 | SUMMARY AND CONCLUSIONS

In this work, a series of parameters were analyzed not only to give some light for explaining the best performance of the chlorinated compound in a recent experimental study by Cui *et al.* but also to examine the behavior of new molecules which are tightly related to synthesized compounds.

Regarding the dipole moment, while the fluorinated system had the lowest dipole values in the gas phase and chloroform, the chlorinated compound presented the lowest value in chlorobenzene. It is a clear solvent dependence of dipole moment. Nonetheless, the brominated system seems to be an attractive compound since it had the lowest dipole moment value compared to all studied molecules and mediums, which is relevant for charge mobility.

All charge transfer descriptors A, χ^+, and ω^+ predicted BTP-4Cl as a better acceptor than BTP-4F, which could be a reason for the outstanding work the photovoltaic device made of PBDB-TF:BTP-4Cl photoactive layer. When solvents are taken into account for the proposed systems, it is observed that BTP-4Br and BTP-4I have similar charge transfer parameter values to BTP-4F and BTP-4Cl; in fact, the brominated system presents slightly higher values than experimental synthesized systems.

Another factor in favor of the better performing of the chlorinated system in comparison with the fluorinated system is the reorganization energy, λ_-, which is smaller for BTP-4Cl than BTP-4F, predicts a lower energy barrier in charge transport. On the other hand, in CF and CB solvents, the theoretically proposed compounds have lower λ_- reorganization energy than synthesized molecules. It is a pleasing result to consider for future research.

Binding energy is another parameter indicating that chlorinated compound has a little better behavior than fluorinated compound in the photoactive layer since E_b is lower for the former, suggesting that exciton is easier dissociated in the chlorinated compound. Additionally, the brominated and iodized proposed systems have even smaller E_b values than the chlorinated system.

The charge separation process is also related to the difference $LUMO_D - LUMO_A$, known as the driving force. This

quantity is more significant for chlorinated than the fluorinated system, which is also in line with the better fulfillment of the former in the experimental study.

The calculated HOMO-LUMO gap is smaller for BTP-4Cl than BTP-4F, which could be seen as a more excellent opportunity to promote an electron to an excited state. The brominated proposed compound presents an even smaller electron gap than synthesized systems.

Clearly, our methodology and Scharber's formula are not describing the experimental open-circuit voltage. From Eq. 1, V_{OC} is related to the difference $\varepsilon_{HOMO}^{donor} - \varepsilon_{LUMO}^{acceptor}$; since LUMO of the chlorinated compound is more negative than LUMO of the fluorinated compound; it is obtained lower V_{OC} for BTP-4Cl system theoretically. Nonetheless, experimental V_{OC} of the chlorinated system was higher than the fluorinated system; an unexpected result even remarked in the experimental study carried out by Cui *et. al.*

In order to get good performance in the photovoltaic device, donor and acceptor materials in the photoactive layer must have complementary absorption spectra, that is, complement each other to absorb the broad spectrum of solar radiation. This condition is well satisfied by BTP-4F and BTP-4Cl acceptors in conjunction with PBDB-TF donor. Actually, the main peak of the chlorinated compound is slightly redshifted concerning the main peak of the fluorinated compound; therefore, the donor-acceptor combination is better for the former since the main peak of the donor is at lower wavelengths, and in this way, donor and acceptor are well-complemented. Consequently, it is another reason for the better execution of chlorinated molecule in the experimental work. Interestingly, the BTP-4Br and BTP-4I proposed molecules have very similar absorption spectra to chlorinated acceptor, which favors a good achievement in using these molecules in this kind of photovoltaic device.

Finally, regarding exciton dissociation and recombination processes, λ_{in}, ΔG_{CR}, and ΔG_{CT} describe correctly the better fulfillment of BTP-4Cl:PBDB-TF photoactive layer, however, k_{CT}/k_{CR} quotients describe a phenomenon where BTP-4F:PBDB-TF performs a more efficient dissociation/recombination process.

As mentioned in previous paragraphs, most of the parameters related to the performance of the solar cell were improved with the chlorinated molecule compared to the fluorinated compound. The chlorinated system presents the best data for most of the parameters associated with the best work of the organic solar cell made by Cui *et al.* Therefore, this theoretical study can help to understand the highest PCE of PBDB-TF:BTP-4Cl combination in comparison with PBDB-TF:BTP-4F combination. Additionally, outstanding results were also obtained for the molecules theoretically proposed with bromine and iodine, since under the analysis of the same electronic structure parameters, stimulating results were found. The change of the halogen atom in the original molecule improves several electronic structure parameters involved in the power conversion efficiency, which could positively impact this kind of organic solar cell. We are sure these results can help in future organic photovoltaic research.

5 | FUNDING INFORMATION

A. R-G. gratefully acknowledges the financial support from CONACyT (Mexico) [Grant No. 741373]. J. G. R-Z. would like to acknowledge the financial support from Universidad de Guadalajara [Pro-SNI-2020].

6 | RESEARCH RESOURCES

The authors would like to acknowledge the computational resources and technical support offered by the Data Analysis and Supercomputing Center (CADS, for its acronym in Spanish) of the University of Guadalajara through *Leo Atrox* supercomputer.

7 | ASSOCIATED CONTENT

Supporting Information

Justification of methodology (XC-functional and basis set choice). Description of electronic parameters used in this study. Validation of the number of monomers used for PBDB-TF polymer calculation.

8 | DATA AVAILABILITY

The raw/processed data required to reproduce these findings cannot be shared at this time due to technical or time limitations. They can be obtained via email to the corresponding author.

references

[1] Bella AP, Panneerselvam M, Vedha SA, Jaccob M, Solomon RV, Merlin JP. DFT-TDDFT framework of diphenylamine based mixed valence compounds for optoelectronic applications–Structural modification of π-acceptors. Computational Materials Science 2019;162:359–369.

[2] Ans M, Iqbal J, Ayub K, Ali E, Eliasson B. Spirobifluorene based small molecules as an alternative to traditional fullerene acceptors for organic solar cells. Materials Science in Semiconductor Processing 2019;94:97–106.

[3] Ganesamoorthy R, Sathiyan G, Sakthivel P. Fullerene based acceptors for efficient bulk heterojunction organic solar cell applications. Solar Energy Materials and Solar Cells 2017;161:102–148.

[4] Ge J, Xie L, Peng R, Fanady B, Huang J, Song W, et al. 13.34% Efficiency Non-Fullerene All-Small-Molecule Organic Solar Cells Enabled by Modulating the Crystallinity of Donors via a Fluorination Strategy. Angewandte Chemie International Edition 2020;59(7):2808–2815.

[5] Abuelwafa A, Dongol M, El-Nahass M, Soga T. Role of Platinum Octaethylporphyrin (PtOEP) in PCPDTBT:PCBM solar cell performance. Journal of Molecular Structure 2020;1202:127303.

[6] Bai RR, Zhang CR, Wu YZ, Shen YL, Liu ZJ, Chen HS. Donor Halogenation Effects on Electronic Structures and Electron Process Rates of donor/C_{60} Heterojunction Interface: A Theoretical Study on F n ZnPc (n= 0, 4, 8, 16) and Cl n SubPc (n= 0, 6). The Journal of Physical Chemistry A 2019;123(18):4034–4047.

[7] Izquierdo MA, Broer R, Havenith RW. Theoretical Study of the Charge Transfer Exciton Binding Energy in Semiconductor Materials for Polymer: Fullerene-Based Bulk Heterojunction Solar Cells. The Journal of Physical Chemistry A 2019;123(6):1233–1242.

[8] Kippelen B, Brédas JL. Organic photovoltaics. Energy & Environmental Science 2009;2(3):251–261.

[9] Dou L, You J, Hong Z, Xu Z, Li G, Street RA, et al. 25th anniversary article: a decade of organic/polymeric photovoltaic research. Advanced Materials 2013;25(46):6642–6671.

[10] Hoppe H, Sariciftci NS. Organic solar cells: An overview. Journal of Materials Research 2004;19(7):1924–1945.

[11] Günes S, Neugebauer H, Sariciftci NS. Conjugated polymer-based organic solar cells. Chemical Reviews 2007;107(4):1324–1338.

[12] Fan Q, Méndez-Romero UA, Guo X, Wang E, Zhang M, Li Y. Fluorinated Photovoltaic Materials for High-Performance Organic Solar Cells. Chemistry–An Asian Journal 2019;14(18):3085–3095.

[13] Li X, Xu Z, Guo X, Fan Q, Zhang M, Li Y. Synthesis and photovoltaic properties of a small molecule acceptor with thienylenevinylene thiophene as π bridge. Dyes and Pigments 2019;160:227–233.

[14] Du X, Heumueller T, Gruber W, Classen A, Unruh T, Li N, et al. Efficient polymer solar cells based on non-fullerene acceptors with potential device lifetime approaching 10 years. Joule 2019;3(1):215–226.

[15] Sun H, Chen F, Chen ZK. Recent progress on non-fullerene acceptors for organic photovoltaics. Materials Today 2019;24:94–118.

[16] Yuan J, Zhang Y, Zhou L, Zhang G, Yip HL, Lau TK, et al. Single-junction organic solar cell with over 15% efficiency using fused-ring acceptor with electron-deficient core. Joule 2019;3(4):1140–1151.

[17] Zhao W, Li S, Yao H, Zhang S, Zhang Y, Yang B, et al. Molecular optimization enables over 13% efficiency in organic solar cells. Journal of the American Chemical Society 2017;139(21):7148–7151.

[18] Kan B, Feng H, Yao H, Chang M, Wan X, Li C, et al. A chlorinated low-bandgap small-molecule acceptor for organic solar cells with 14.1% efficiency and low energy loss. Science China Chemistry 2018;61(10):1307–1313.

[19] Zhang H, Yao H, Hou J, Zhu J, Zhang J, Li W, et al. Over 14% efficiency in organic solar cells enabled by chlorinated nonfullerene small-molecule acceptors. Advanced Materials 2018;30(28):1800613.

[20] Cui Y, Yao H, Zhang J, Zhang T, Wang Y, Hong L, et al. Over 16% efficiency organic photovoltaic cells enabled by a chlorinated acceptor with increased open-circuit voltages. Nature Communications 2019;10(1):1–8.

[21] Che X, Li Y, Qu Y, Forrest SR. High fabrication yield organic tandem photovoltaics combining vacuum-and solution-processed subcells with 15% efficiency. Nature Energy 2018;3(5):422–427.

[22] Yong X, Zhang J. Theoretical investigations for organic solar cells. Materials Technology 2013;28(1-2):40–64.

[23] Khan M, Jilani F, Ayub A, Naseem Z, Ayub AR, Mahr MS, et al. Designing of cyanobenzene based small molecules with suitable photovoltaic parameters for organic solar cells. International Journal of Quantum Chemistry 2021;121(15):e26673.

[24] Xu X, Zheng S. Designing new donor materials based on functionalized DCCnT with different electron-donating groups: A density functional theory (DFT) and time dependent density functional theory (TDDFT)-based study. International Journal of Quantum Chemistry 2020;120(8):e26112.

[25] Moncada JL, Toro-Labbé A. A theoretical study of conducting oligomeric systems: The conceptual DFT perspective. Chemical Physics Letters 2006;429(1-3):161–165.

[26] Borsenberger PM, Fitzgerald JJ. Effects of the dipole moment on charge transport in disordered molecular solids. The Journal of Physical Chemistry 1993;97(18):4815–4819.

[27] Cisneros-García Z, Hernández DA, Tenorio FJ, Rodríguez-Zavala J. Electronic structure of hydroxylated La@C_{82} endohedral metallofullerene: implications on photovoltaic cells. Molecular Physics 2020;118(14):e1705411.

[28] Knupfer M. Exciton binding energies in organic semiconductors. Applied Physics A 2003;77(5):623–626.

[29] Brédas JL, Cornil J, Heeger AJ. The exciton binding energy in luminescent conjugated polymers. Advanced Materials 1996;8(5):447–452.

[30] Scharber MC, Mühlbacher D, Koppe M, Denk P, Waldauf C, Heeger AJ, et al. Design rules for donors in bulk-heterojunction solar cells—Towards 10% energy-conversion efficiency. Advanced Materials 2006;18(6):789–794.

[31] Pan QQ, Li SB, Wu Y, Sun GY, Geng Y, Su ZM. A comparative study of a fluorene-based non-fullerene electron acceptor and $PC_{61}BM$ in an organic solar cell at a quantum chemical level. RSC Advances 2016;6(84):81164–81173.

[32] Faist MA, Kirchartz T, Gong W, Ashraf RS, McCulloch I, de Mello JC, et al. Competition between the charge transfer state and the singlet states of donor or acceptor limiting the efficiency in polymer:fullerene solar cells. Journal of the American Chemical Society 2012;134(1):685–692.

[33] Heyd J, Scuseria GE, Ernzerhof M. Hybrid functionals based on a screened Coulomb potential. The Journal of Chemical Physics 2003;118(18):8207–8215.

[34] Ditchfield R, Hehre WJ, Pople JA. Self-consistent molecular-orbital methods. IX. An extended Gaussian-type basis for molecular-orbital studies of organic molecules. The Journal of Chemical Physics 1971;54(2):724–728.

[35] Weigend F, Ahlrichs R. Balanced basis sets of split valence, triple zeta valence and quadruple zeta valence quality for H to Rn: Design and assessment of accuracy. Physical Chemistry Chemical Physics 2005;7(18):3297–3305.

[36] Weigend F. Accurate Coulomb-fitting basis sets for H to Rn. Physical Chemistry Chemical Physics 2006;8(9):1057–1065.

[37] Marenich AV, Cramer CJ, Truhlar DG. Universal solvation model based on solute electron density and on a continuum model of the solvent defined by the bulk dielectric constant and atomic surface tensions. The Journal of Physical Chemistry B 2009;113(18):6378–6396.

[38] Frisch M, Trucks G, Schlegel H, Scuseria G, Robb M, Cheeseman J, et al. Gaussian 16. Revision A 2016;3.

[39] Lu T, Chen F. Multiwfn: a multifunctional wavefunction analyzer. Journal of Computational Chemistry 2012;33(5):580–592.

[40] Xie X, Liu Y, Zhao L, Zhao X. The effects of electronic and structural properties of two small molecules on their photovoltaic performances. Chemical Physics Letters 2019;728:37–43.

[41] Liu Z, Wu Y, Zhang Q, Gao X. Non-fullerene small molecule acceptors based on perylene diimides. Journal of Materials Chemistry A 2016;4(45):17604–17622.

[42] Pauling L. The nature of the chemical bond. IV. The energy of single bonds and the relative electronegativity of atoms. Journal of the American Chemical Society 1932;54(9):3570–3582.

[43] Imahori H, Tkachenko NV, Vehmanen V, Tamaki K, Lemmetyinen H, Sakata Y, et al. An extremely small reorganization energy of electron transfer in Porphyrin-Fullerene Dyad. The Journal of Physical Chemistry A 2001;105(10):1750–1756.

[44] Chen HY, Chao I. Effect of perfluorination on the charge-transport properties of organic semiconductors: density functional theory study of perfluorinated pentacene and sexithiophene. Chemical Physics Letters 2005;401(4-6):539–545.

[45] Nunzi JM. Organic photovoltaic materials and devices. Comptes Rendus Physique 2002;3(4):523–542.

[46] Su YW, Lan SC, Wei KH. Organic photovoltaics. Materials Today 2012;15(12):554–562.

[47] Rauh D, Wagenpfahl A, Deibel C, Dyakonov V. Relation of open circuit voltage to charge carrier density in organic bulk heterojunction solar cells. Applied Physics Letters 2011;98(13):69.

[48] Harder JW, Fontenla JM, Pilewskie P, Richard EC, Woods TN. Trends in solar spectral irradiance variability in the visible and infrared. Geophysical Research Letters 2009;36(7):L07801.

[49] Marcus RA. On the theory of oxidation-reduction reactions involving electron transfer. The Journal of Chemical Physics 1956;24(5):966–978.

[50] Yin S, Lv Y. Modeling hole and electron mobilities in pentacene ab-plane. Organic Electronics 2008;9(5):852–858.

[51] Cornil J, Brédas JL, Zaumseil J, Sirringhaus H. Ambipolar transport in organic conjugated materials. Advanced Materials 2007;19(14):1791–1799.

[52] Marcus RA. Electron transfer reactions in chemistry: theory and experiment. Journal of Electroanalytical Chemistry 1997;438(1-2):251–259.

[53] Rana D, Materny A. Effect of static external electric field on bulk and interfaces in organic solar cell systems: A density-functional-theory-based study. Spectrochimica Acta Part A: Molecular and Biomolecular Spectroscopy 2021;253:119565.

[54] Ans M, Iqbal J, Eliasson B, Saif MJ, Javed HMA, Ayub K. Designing of non-fullerene 3D star-shaped acceptors for organic solar cells. Journal of Molecular Modeling 2019;25(5):1–12.

[55] Li Y, Pullerits T, Zhao M, Sun M. Theoretical characterization of the PC_{60}BM:PDDTT model for an organic solar cell. The Journal of Physical Chemistry C 2011;115(44):21865–21873.

Figures and Tables

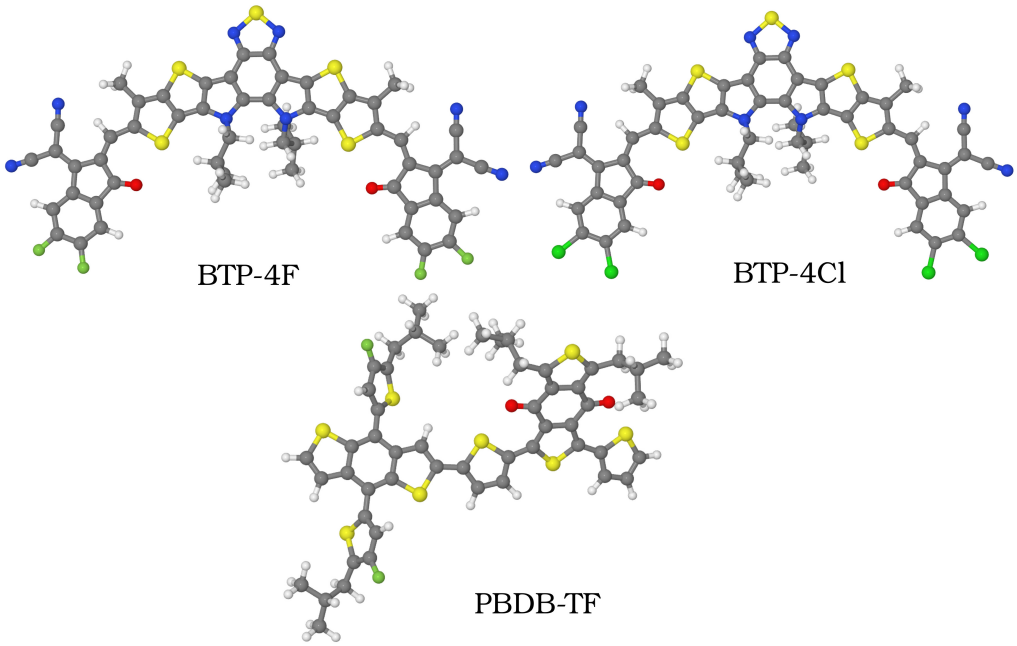

FIGURE 1 Three-dimensional molecular structures of the BTP-4F and BTP-4Cl acceptors, as well as one unit of the PBDB-TF donor polymer.

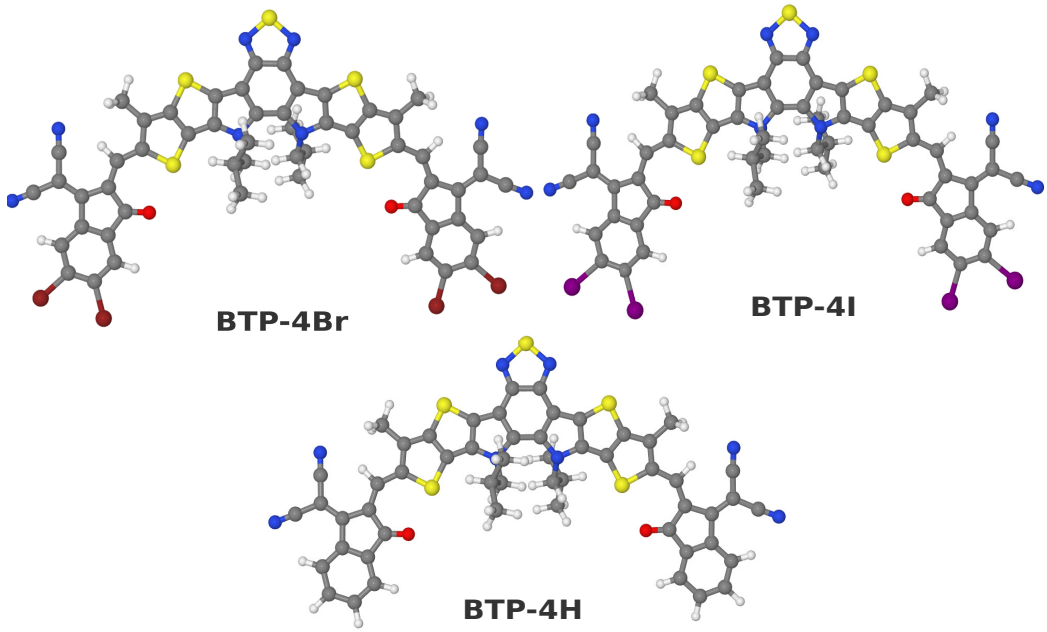

FIGURE 2 Three-dimensional molecular structures of the proposed BTP-4Br/BTP-4I acceptors and the dehalogenated BTP-4H acceptor.

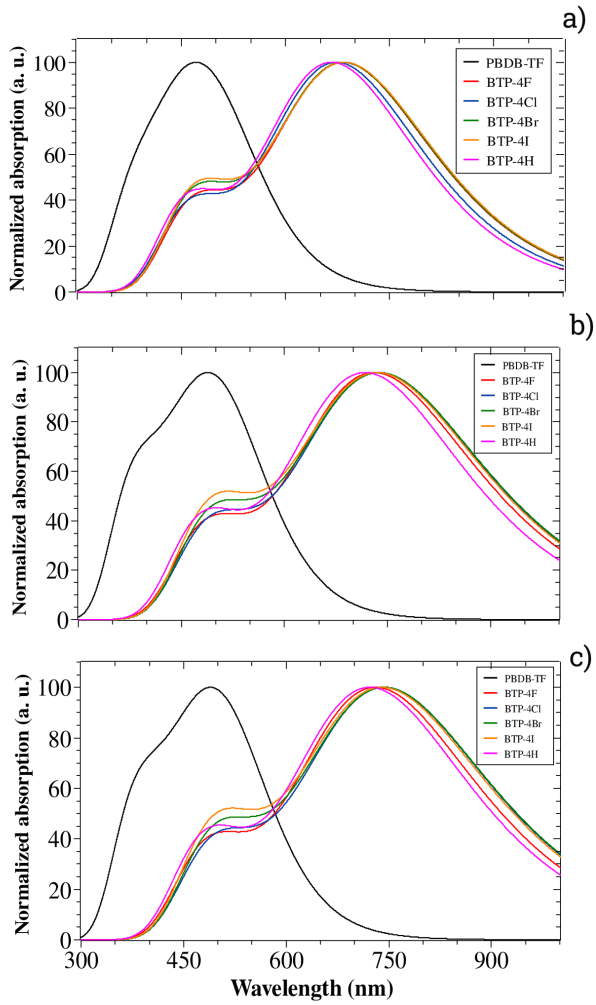

FIGURE 3 Normalized simulated UV-Vis spectra for all the analyzed compounds in a) gas phase, b) chloroform, and c) chlorobenzene.

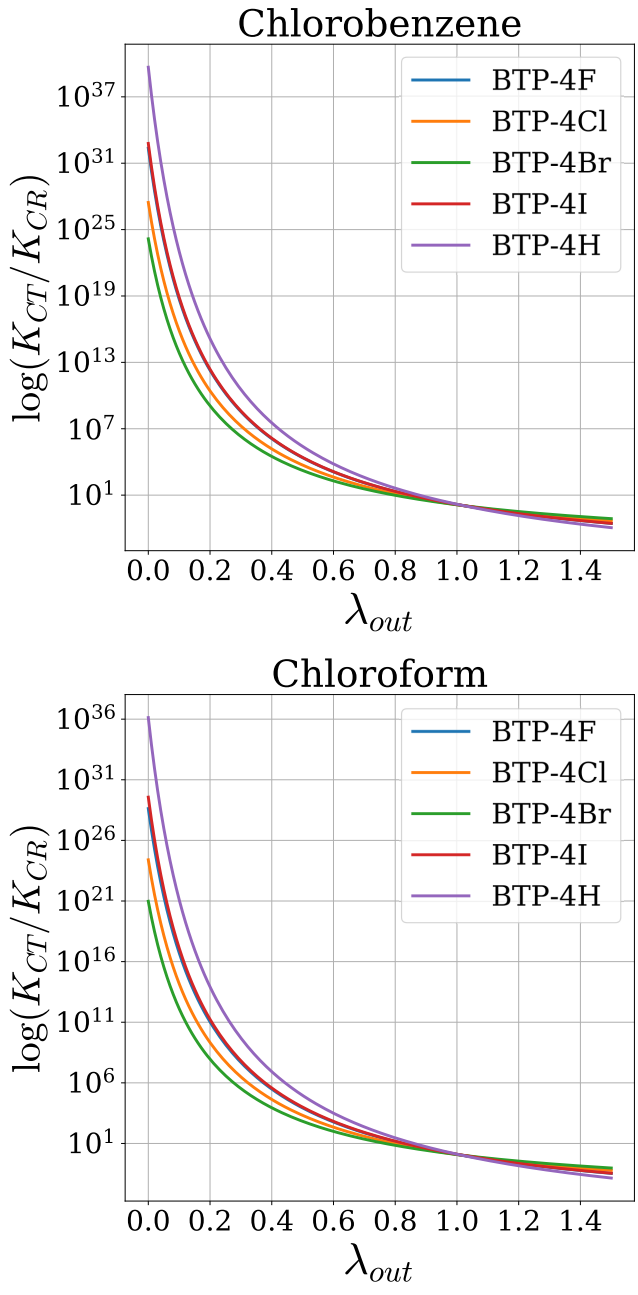

FIGURE 4 $\log(k_{CT}/k_{CR})$ as a function of λ_{out} taking into account chlorobenzene and chloroform solvents.

TABLE 1 Dipole moment calculated for all the molecules in gas phase (GP), chloroform (CF), and chlorobenzene (CB). Units in Debye.

Molecule	GP	CF	CB
BTP-4F	1.395	2.116	2.452
BTP-4Cl	0.624	2.022	2.771
BTP-4Br	0.404	0.274	0.382
BTP-4I	1.231	3.683	3.537
BTP-4H	5.684	8.992	8.314
PBDB-TF	1.192	1.601	1.648

TABLE 2 Accepting (A, χ^+, and $\bar{\omega}^+$)[a]-Donating (I, χ^-, and $\bar{\omega}^-$)[b] properties (eV) for the studied molecules in gas phase (GP), chloroform (CF), and chlorobenzene (CB).

Solvent	Molecule	I	A	χ^-	χ^+	$\bar{\omega}^-$	$\bar{\omega}^+$
GP	BTP-4F	6.68	3.08	23.12	15.92	9.28	4.40
	BTP-4Cl	6.70	3.16	23.25	16.18	9.65	4.63
	BTP-4Br	6.59	3.04	22.81	15.72	9.17	4.36
	BTP-4I	6.57	3.04	22.74	15.68	9.15	4.35
	BTP-4H	6.45	2.81	22.17	14.88	8.43	3.80
	PBDB-TF	6.35	1.67	20.71	11.36	5.73	1.73
CF	BTP-4F	5.50	3.63	20.12	16.37	13.51	8.95
	BTP-4Cl	5.53	3.69	20.27	16.60	13.98	9.37
	BTP-4Br	5.53	3.69	20.29	16.61	13.96	9.35
	BTP-4I	5.48	3.64	20.09	16.41	13.70	9.14
	BTP-4H	5.43	3.54	19.83	16.05	13.00	8.51
	PBDB-TF	5.38	2.77	18.92	13.69	8.56	4.48
CB	BTP-4F	5.44	3.64	19.97	16.37	13.84	9.30
	BTP-4Cl	5.49	3.71	20.17	16.60	14.26	9.67
	BTP-4Br	5.48	3.71	20.16	16.61	14.30	9.71
	BTP-4I	5.43	3.66	19.96	16.41	14.02	9.47
	BTP-4H	5.39	3.56	19.72	16.07	13.31	8.84
	PBDB-TF	5.35	2.81	18.85	13.77	8.74	4.67

[a]The higher this value, the better the acceptor capacity.

[b]The lower this value, the better the donor capacity.

TABLE 3 Reorganization energies for holes and electrons (eV) in the six studied molecules (with and without solvents). GP = gas phase, CF = chloroform, and CB = chlorobenzene.

Solvent	Molecule	λ_+	λ_-
	BTP-4F	0.174	0.134
	BTP-4Cl	0.170	0.123
GP	BTP-4Br	0.166	0.126
	BTP-4I	0.164	0.126
	BTP-4H	0.164	0.135
	PBDB-TF	0.233	0.287
	BTP-4F	0.163	0.111
	BTP-4Cl	0.157	0.104
CF	BTP-4Br	0.157	0.101
	BTP-4I	0.157	0.102
	BTP-4H	0.159	0.112
	PBDB-TF	0.294	0.297
	BTP-4F	0.163	0.109
	BTP-4Cl	0.151	0.103
CB	BTP-4Br	0.157	0.099
	BTP-4I	0.155	0.102
	BTP-4H	0.161	0.112
	PBDB-TF	0.239	0.302

TABLE 4 Exciton binding energy for all the studied molecules (with and without solvents). GP = gas phase, CF = chloroform, and CB = chlorobenzene.

	E_b (eV)		
Molecule	GP	CF	CB
BTP-4F	2.62	2.60	2.60
BTP-4Cl	2.60	2.57	2.57
BTP-4Br	2.57	2.54	2.54
BTP-4I	2.57	2.54	2.53
BTP-4H	2.63	2.60	2.59
PBDB-TF	2.85	2.98	2.97

TABLE 5 Frontier molecular orbital energies (eV) calculated at HSE/6-311G(d,p) level of theory and experimental results[a].

Molecule	HOMO	$HOMO^{exp}$	LUMO	$LUMO^{exp}$	E_g	E_g^{exp}
BTP-4F	-5.69	-5.65	-4.02	-4.02	1.67	1.63
BTP-4Cl	-5.73	-5.68	-4.08	-4.12	1.65	1.56
PBDB-TF	-5.22	-5.45	-2.85	-3.64	2.37	1.81

[a] Cui *et al.* [20].

TABLE 6 Estimated V_{OC} for the two donor-acceptor combinations and experimental V_{OC} reported by Cui *et al.*

Combination	V_{oc} (V)	V_{oc}^{exp} (V)
BTP-4F:PBDB-TF	0.90	0.83
BTP-4Cl:PBDB-TF	0.84	0.87

TABLE 7 Energy of frontier molecular orbitals (eV) for the six analyzed molecules (with and without solvents). GP = gas phase, CF = chloroform, and CB = chlorobenzene.

Solvent	Molecule	HOMO	LUMO	E_g
	BTP-4F	-5.69	-4.02	1.67
	BTP-4Cl	-5.73	-4.08	1.65
GP	BTP-4Br	-5.71	-4.09	1.62
	BTP-4I	-5.70	-4.05	1.65
	BTP-4H	-5.55	-3.88	1.67
	PBDB-TF	-5.22	-2.85	2.37
	BTP-4F	-5.39	-3.75	1.64
	BTP-4Cl	-5.42	-3.80	1.62
CF	BTP-4Br	-5.42	-3.84	1.58
	BTP-4I	-5.38	-3.75	1.63
	BTP-4H	-5.32	-3.67	1.65
	PBDB-TF	-5.26	-2.85	2.41
	BTP-4F	-5.37	-3.73	1.64
	BTP-4Cl	-5.40	-3.78	1.62
CB	BTP-4Br	-5.40	-3.82	1.58
	BTP-4I	-5.36	-3.73	1.63
	BTP-4H	-5.31	-3.65	1.66
	PBDB-TF	-5.27	-2.85	2.42

TABLE 8 Estimated V_{oc} for the five donor-acceptor combinations in gas phase and in presence of solvents. GP = gas phase, CF = chloroform, and CB = chlorobenzene.

	V_{oc} (V)		
Combination	GP	CF	CB
BTP-4F:PBDB-TF	0.90	1.21	1.24
BTP-4Cl:PBDB-TF	0.84	1.16	1.19
BTP-4Br:PBDB-TF	0.83	1.12	1.15
BTP-4I:PBDB-TF	0.87	1.21	1.24
BTP-4H:PBDB-TF	1.04	1.29	1.32

TABLE 9 Characteristics of the main absorption peaks of BTP-4F and BTP-4Cl acceptor molecules in UV-Vis region (gas phase - HSE/6-311G**) and experimental data.

Molecule	λ_{max}^{exp} (nm)	λ (nm)	E_{opt}^{exp} (eV)	f	Main configuration
BTP-4F	732	679.38	1.407	1.99	H→L(100 %)
		602.67		0.055	H-1→L(12 %), H→L+1(86 %)
		525.25		0.158	H→L+2(97 %)
BTP-4Cl	746	689.90	1.400	2.04	H→L(100 %)
		610.09		0.06	H-1→L(12 %), H→L+1(86 %)
		534.35		0.16	H→L+2(98 %)

TABLE 10 Characteristics of the main absorption peaks of the five acceptor molecules in the UV-Vis region (gas phase).

Molecule	λ (nm)	f	Main configuration
BTP-4F	679.38	1.99	H→L(100 %)
	602.67	0.055	H-1→L(12 %), H→L+1(86 %)
	525.25	0.158	H→L+2(97 %)
BTP-4Cl	689.90	2.04	H→L(100 %)
	610.09	0.060	H-1→L(12 %), H→L+1(86 %)
	534.35	0.160	H→L+2(98 %)
BTP-4Br	690.38	2.01	H→L(100 %)
	610.59	0.069	H-1→L(11 %), H→L+1(86 %)
	534.47	0.160	H→L+2(97 %)
BTP-4I	692.06	2.02	H→L(100 %)
	610.21	0.071	H-1→L(12 %), H→L+1(86 %)
	533.63	0.162	H→L+2(97 %)
BTP-4H	672.12	1.97	H→L(100 %)
	595.82	0.063	H-1→L(13 %), H→L+1(86 %)
	513.50	0.142	H→L+2(97 %)

TABLE 11 Characteristics of the main absorption peaks of the five acceptor molecules in the UV-Vis region (chloroform).

Molecule	λ (nm)	f	Main configuraion
BTP-4F	732.56	2.340	H→L(100 %)
	624.04	0.109	H-2→L(2 %), H-1→L(3 %), H→L+1(93 %)
	536.99	0.168	H→L+2(98 %)
BTP-4Cl	745.91	2.370	H→L(100 %)
	634.52	0.111	H-2→L(4 %), H→L+1(93 %)
	550.62	0.173	H→L+2(98 %)
BTP-4Br	747.50	2.307	H→L(100 %)
	636.57	0.125	H-2→L(3 %), H→L+1(93 %)
	553.49	0.174	H→L+2(98 %)
BTP-4I	745.22	2.319	H→L(100 %)
	631.19	0.148	H-2→L(3 %), H-1→L(3 %), H→L+1(93 %)
	544.29	0.173	H→L+2(98 %)
BTP-4H	724.78	2.296	H→L(100 %)
	616.17	0.132	H-2→L(2 %), H-1→L(3 %), H→L+1(93 %)
	524.29	0.149	H→L+2(98 %)

TABLE 12 Characteristics of the main absorption peaks of the five acceptor molecules in the UV-Vis region (chlorobenzene).

Molecule	λ (nm)	f	Main configuration
BTP-4F	737.89	2.377	H→L(100 %)
	626.41	0.118	H-2→L(2 %), H-1→L(3 %), H→L+1(94 %)
	536.36	0.172	H→L+2(98 %)
BTP-4Cl	751.76	2.409	H→L(100 %)
	637.38	0.121	H-2→L(3 %), H→L+1(94 %)
	550.66	0.178	H→L+2(98 %)
BTP-4Br	753.19	2.335	H→L(100 %)
	639.46	0.136	H-2→L(3 %), H→L+1(94 %)
	553.33	0.177	H→L+2(98 %)
BTP-4I	750.38	2.346	H→L(100 %)
	633.62	0.163	H-2→L(2 %), H-1→L(3 %), H→L+1(94 %)
	543.67	0.178	H→L+2(98 %)
BTP-4H	729.96	2.325	H→L(100 %)
	618.54	0.145	H-2→L(2 %), H-1→L(3 %), H→L+1(94 %)
	524.03	0.003	H-2→L(41 %), H-1→L(59 %)

TABLE 13 Exciton dissociation and recombination parameters (eV) for all the five combinations in gas phase (GP), chloroform (CF), and chlorobenzene (CB).

Solvent	Combination	λ_{in}	ΔG_{CR}	ΔE_{0-0}	ΔG_{CT}	k_{CT}/k_{CR}
GP	BTP-4F:PBDB-TF	0.189	-1.20	2.40	-1.17	21.72
	BTP-4Cl:PBDB-TF	0.183	-1.14	2.40	-1.23	6.81×10^{-5}
	BTP-4Br:PBDB-TF	0.349	-1.13	2.40	-1.24	5.91×10^{-3}
	BTP-4I:PBDB-TF	0.349	-1.17	2.40	-1.20	2.47×10^{-1}
	BTP-4H:PBDB-TF	0.353	-1.34	2.40	-1.03	1.51×10^{6}
CF	BTP-4F:PBDB-TF	0.184	-1.51	2.39	-0.90	4.19×10^{28}
	BTP-4Cl:PBDB-TF	0.181	-1.46	2.39	-0.95	2.50×10^{24}
	BTP-4Br:PBDB-TF	0.178	-1.42	2.39	-0.99	9.53×10^{20}
	BTP-4I:PBDB-TF	0.179	-1.51	2.39	-0.90	3.68×10^{29}
	BTP-4H:PBDB-TF	0.184	-1.59	2.39	-0.82	1.35×10^{36}
CB	BTP-4F:PBDB-TF	0.178	-1.54	2.39	-0.88	2.28×10^{32}
	BTP-4Cl:PBDB-TF	0.178	-1.49	2.39	-0.93	2.85×10^{27}
	BTP-4Br:PBDB-TF	0.174	-1.45	2.39	-0.97	1.47×10^{24}
	BTP-4I:PBDB-TF	0.176	-1.54	2.39	-0.88	6.14×10^{32}
	BTP-4H:PBDB-TF	0.180	-1.62	2.39	-0.80	4.76×10^{39}